Optical Fiber Technology **5**, 338-348 (1999)
Article ID ofte.1999.0286, available online at http://www.idealibrary.com on IDEAL®

Failure Case Study for Optical Fiber Breaks in Metal Packages

Hirotoshi Nagata and Naoki Mitsugi

Optoelectronics Research Division, New Technology Research Laboratories, Sumitomo Osaha Cement Co., Ltd., 585 Toyotomi-cho, Funabashi-shi Chiba 274-8601, Japan

and

Kaori Shima

Advanced Materials Research Division,New Technology Research Laboratories, Sumitomo Osaka Cement Co., Ltd., 585 Toyotomi-cho, Funabashi-shi, Chiba 274-8601, Japan

Received October 21, 1998

A possible cause for optical fiber breaks occurring in hermetically sealed metal packages is examined. Although the fiber itself is screened before use, the potential for fiber breakage still exists since the fiber is installed, slightly bent, in order to accommodate thermal expansion of the package. As a means of screening out devices with possible fiber defects, we propose incorporating into the standard screening process a low-temperature storage test in which thermal shrinkage of the package intensifies bending strain on the fiber, thereby accelerating the failure and identification of fragile de - vices

1. INTRODUCTION

In fiber optic devices, a break in assembled fibers constitutes a catastrophic failure and must be prevented by all means. In hermetically sealed packages, all polymer coatings of the fiber are removed mechanically and the glass surface is metallized by an electroless plating technique before the fiber is soldered onto the metal package [1, 2]. In comparison to unmetallized fibers, metallized fibers cannot withstand as much bending deformation (buckling). For instance, 5-mm-long metallized polarization-maintaining fibers (PMF) buckled and broke when they were

l068-5200/99 $30.00

com~ressed by a distance of 0.75 mm [3]. This critical failure value corresponds to an estimated bending radius of 0.505 mm and an estimated bending strain of 12.4%. Such a high level of strain is never applied to fibers in actual devices. Thus, ordinarily, the mechanical reliability of these device can be ensured [1, 4].

On rare occasions, however, unforeseen failures may occur in devices leading to a serious problem. For instance, as reported in Section 2, a metallized fiber broke at a very low strain level of less than 0.2%. Prior to installation, this fiber had been screened through a bending test with approximately 1 % strain, and the device had also undergone and passed a temperature cycle test. After reviewing the failure analysis results of this unusual fiber break, we conclude that a screening test including low-temperature storage can weed out devices with weakened fibers. Because fiber buckling and deformation intensify at lower temperatures, the proposed simple storage test can accelerate the phenomena by inducing added strain. In our study, we used a stainless steel package because the large difference between the thermal expansion coefficient of the package material and that of the fiber induces intensified fiber buckling. Since stainless steel packages are used for $LiNbO_3$ optical modulators, optical connectors, etc., the results of our study will be applicable in determining the mechanical reliability of these devices.

2. A FAILURE CASE STUDY

Figure 1 shows a photograph of a fiber break found in a fiber feedthrough pipe of the stainless steel optical modulator package. This break occurred during a storage test of the device at decreased temperature (about 0°C). The left- and right-hand sections of the fiber are fixed to the pipe with solder and an epoxy,

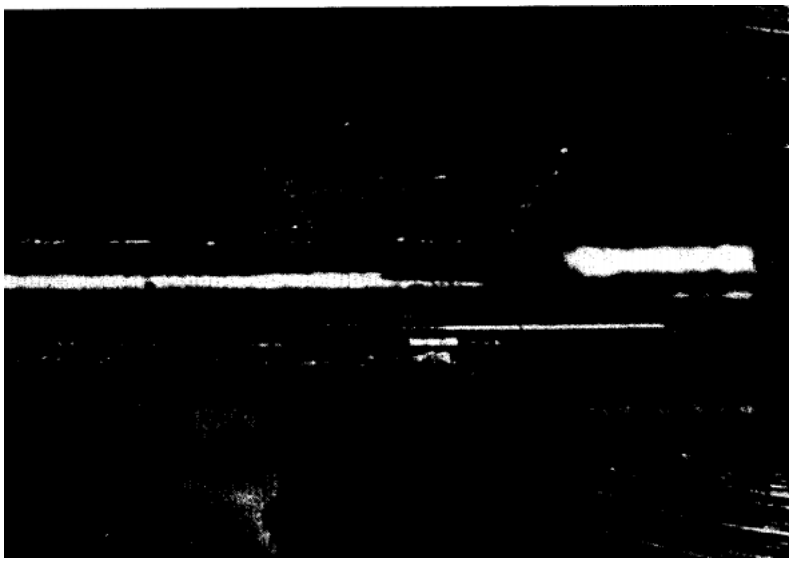

FIG. 1. Example of fiber break failure in the optical device package. The fiber jacket was removed and the surface was metallized before its assembly.

respectively (not shown in the photograph). The length of the fiber between the fixed points was designed to be 5 mm but measured 5.25 mm in this defective sample. The break was located close to the center of the fiber (2.79 mm from the soldered position). As shown, axes of the broken fiber pair were mutually separated by approximately 60 μm, indicating that the fiber within the pipe had been curved slightly. Then, because the break position was at the center of the fiber, the deflection of bent fiber through the 5.25 mm span was estimated to be 30 μm. The magnitude of this deflection was consistent with the value designed for the present package structure, which allowed the fiber to adapt to the thermal elongation of the metal pipe. Using these parameters, we geometrically calculated the bending radius and fiber strain to have been 115 mm and 0.0545% (tensile strain), respectively. Although shrinkage of the metal pipe at decreased temperatures adds additional strain onto the fiber, the total strain was calculated to be only 0.165%. The above estimated residual strain is much less than the level of strain used to screen commercial fibers (approx.1.0%). Furthermore, because the jacket removing and metallization processes opened up the possibility of fiber surface damage, the fibers underwent a bending test (approx. 5 mm radius, 1.25% bending strain) before use. Finally, the devices were screened again by a temperature cycle test between - 20 and + 70°C. The device in question passed all these screening tests, but its fiber broke during its use at only 0°C.

Figure 2 shows a secondary electron microscopic (SEM) image of the fractured surface of the broken polarization maintaining fiber. The fiber surface was coated

FIG. 2. SEM image of the fractured surface of the broken polarization-maintaining fiber of Fig. 1. The fiber surface was coated with an Au/Ni binary layer.

by an Au/Ni binary layer. The right side of the fractured surface, showing chipped fiber elements, corresponds to the concave region of the bent fiber; a compressive strain was applied by bending. The opposite side of the fractured surface is very smooth, Iike a mirror face in a common fractograph. A specific origin of fracture origin, such as a flaw [5], could not be found at the edge of this mirrorlike region. A remarkable feature of this fractured surface is a meltlike inclusion found in the region and near its edge, which is magnified in Fig. 3. The size of the inclusion is approximately 10 μm × 5 μm (the depth was not known). In Fig. 3, the results of chemical analyses through the SEM are also shown: a planar distribution of Ni, C, and Cl contents. In addition to a SiO_2 matrix, slightly greater amounts of carbon and chlorine were detected in the inclusion. Because the concentration of such impurities was negligible, the inclusion was deduced to be a SiO_2-based material rather than an extrinsic contamination. The cause for the inclusion was not known, but it is probable that a SiO_2 chip slightly rich in C1 was trapped in the material during some process using $SiC1_4$ or $C1_2$. If the inclusion came from an extrinsic contamination such as graphite or metal, the mechanical strength of the fiber would have deteriorated greatly and the anomaly would have been found through the usual screening tests.

Although we unfortunately could not identify the origin of the fiber break, all such possible failures must be identified and screened out completely before fibers are set up for actual use. The only difference between the common screening tests and the incidence of failure was the duration that a certain magnitude of strain was applied to the fiber. The particular device was kept for more than half an hour at 0°C before the fiber break; the amount of time in which strain was applied to the fiber during the screening tests was shorter. Further, there is a possibility that a twistlike strain applied to the fiber in the actual device. We speculate here that a continuous amount of strain was applied to the fiber, including the anomaly, until it ultimately broke, despite the fact that it had endured the short-term application of strain during screening.

3. PROPOSAL OF STRAIN-ACCELERATED SCREENING TESTS

In order to screen unexpectedly vulnerable fibers, we propose a low-temperature storage test, in which fiber breakage is accelerated by increased strain. In some optical waveguide devices, the fibers are not tautly installed but rather compressed toward the waveguide element intentionally to prevent excessive fiber tension at elevated temperatures (e.g. 80°C as a common storage temperature) [6-8]. The fiber is thus allowed to extend and adjust itself to a larger thermal expansion of the package material. At decreased temperatures, however, due to notable thermal shrinkage of the package, the installed fiber buckles from further compression. Such buckling induces strain within the fiber, causing weak fibers to break as mentioned in the previous section.

At first, to estimate the magnitude of strain in the fiber due to buckling, we consider a straight fiber with length L to be compressed along the axis by a

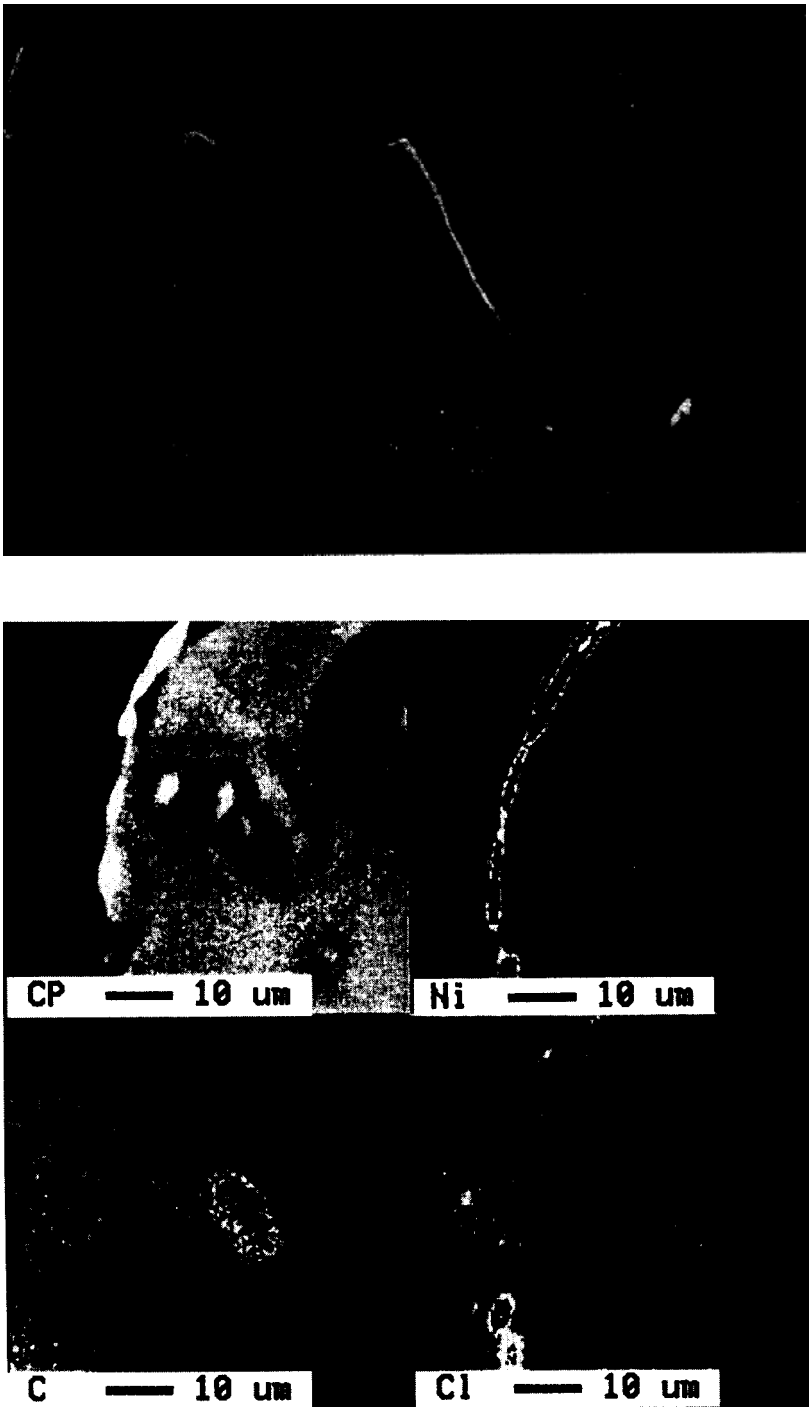

Fig. 3. A magnified SEM image of the inclusion found in Fig. 2. The other images show planar distributions of Ni, C, and Cl elements detected from the fractured surface. The Ni was detected from the Au/Ni metallization layer on the fiber. The image denoted by "CP" shows a information of chemical composition: a region of a darker contrast includes elements lighter than SiO_2.

distance ΔL. Because the ends of the fiber are fixed solidly to a waveguide element and to the fiber-insertion port of a package, the fiber is expected to bend in a wavelike pattern between the distance of (L - ΔL): the wavelength of this deformed section of the fiber is (L - ΔL). In such situation, the curve of the bent fiber is replaced by an arc of a circle with radius R, and the geometric relationship among L, ΔL, and R can be expressed by the formula

$$\Delta L = L - 4R \sin (L / 4R). \tag{1}$$

Here, the lengths of the arc and the chord are calculated as $L/2$ and (L - ΔL)/2, respectively.

Then, in order to examine how decreased temperatures contributes to the fiber buckling, using the thermal expansion coefficient a of the package material and the temperature change AT from the original temperature when the fiber was straight, A L is expressed as

$$\Delta L = \alpha L \, |\Delta T|. \tag{2}$$

Because only the package shrinkage is accounted for and ΔL is determined by Eq. (1) as the decrease in the length, the absolute of ΔT is used (the temperature change is actually a negative value). Here, because the a for the glass fiber is smaller than that of conventional package materials, the fiber length change is neglected. From Eqs. (1) and (2), the ΔT dependency of R is obtained from

$$\alpha \, |\Delta T| = 1 - (4R / L) \sin (L / 4R). \tag{3}$$

On the other hand, a tensile strain s (%) generated by this bending on the fiber is approximately derived by

$$s = [(0.125/2) /R] \times 100, \tag{4}$$

in which 0.125 corresponds to the diameter of the fiber in millimeters.

Figures 4 and 5 shows calculation results for the fiber bending radius R and the induced tensile strain s, respectively, as functions of the temperature change ΔT. In the calculation, the α of stainless steel, I .46× 10^{-5} was used because stainless steel is the package material used for $LiNbO_3$ optical modulators, optical connectors, etc. Further, a dependency of the results on the initial fiber length L, varying from 3 to 30 mm, was examined and shown in the same figures. Similar calculation results are shown in Figs. 6 and 7 as a relationship between R vs L, and s vs L, respectively. The results clearly indicate that the shorter the initial fiber length, the greater the effect of the temperature decrease in inducing a larger bending strain on the fiber.

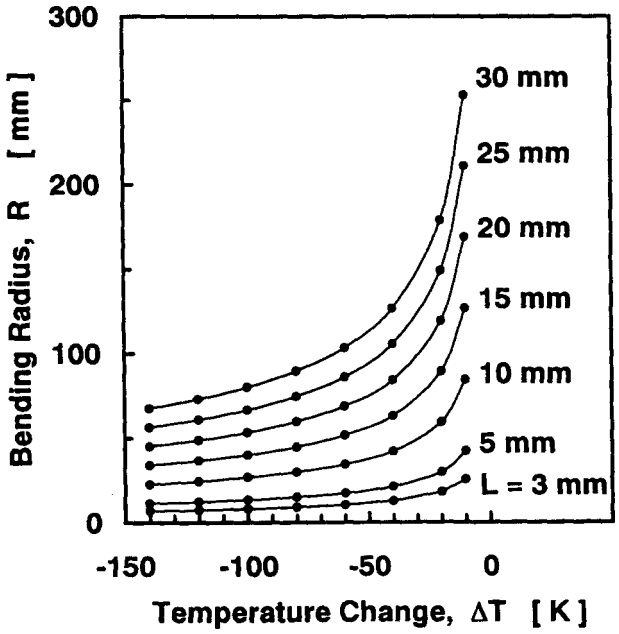

FIG. 4. Calculation result of the fiber bending radius R as a function of the temperature change ΔT.

Even at an ordinary device operation temperature of 40°C, the fibers that are initially installed with an intentional bend to cancel the package expansion at 80°C are strained already at the level shown by the point for $\Delta T = -40$ K in Figs. 5 and 7. These residual strains are calculated to be 0.30, 0.099, and 0.059% for the 5-mm, 15-mm and 25-mm-long fibers, respectively. Because the common device storage temperature is -40°C, the similar strain reaches 0.51, 0.19, and 0.10% for the 5-mm 15-mm, and 25-mm-long fibers, respectrvely. It is noted that such estimated strains are lower than screening strain for recent commercial fibers (approx. 1.0%), suggesting that the fibers can endure bending strains caused by package structures. However, as shown in Section 2, a possibility of the break of such strained fibers is not zero due to unforeseen failures in the installed fibers.

A temperature cycle test and/or a high temperature storage test are commonly rformed in order to identify those devices that may fail at elevated temperatures. PHeowever these standard tests cannot accelerate fiber breakage, because the residual strain in the bent fiber is smaller at higher temperatures. Thus, a low-temperature storage test is preferable for the purpose of identifying devices with weak fibers, in which fiber break failure is accelerated by added strain.

Concerning a continuous application of the different amount of stresses of σ_1 and σ_2 to the material, there is a simple relationship with respect to the corresponding duration t_1 and t_2 that the stress is applied:

$$\sigma_1^n t_1 = \sigma_2^n t_2. \tag{5}$$

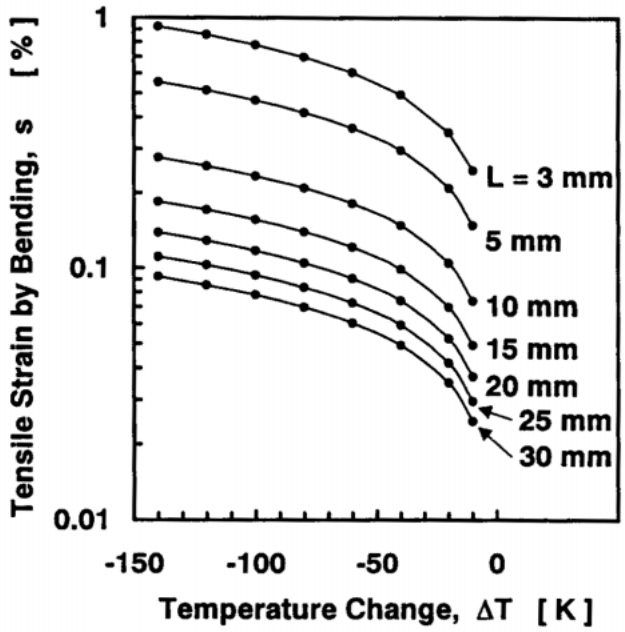

FIG. 5. Caleulation results of the induced tensile strain s as a function of the temperature change **Δ***T*.

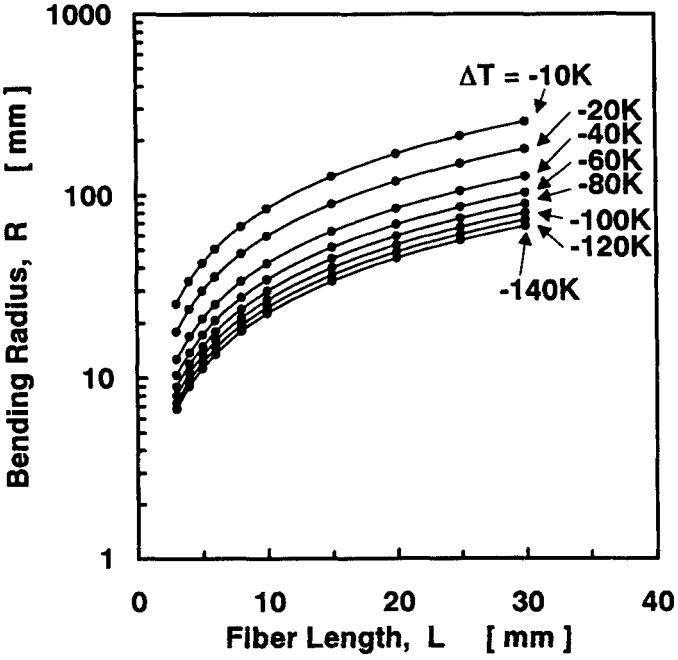

FIG. 6. A relationship between *R* and *L* replotted from Fig. 4.

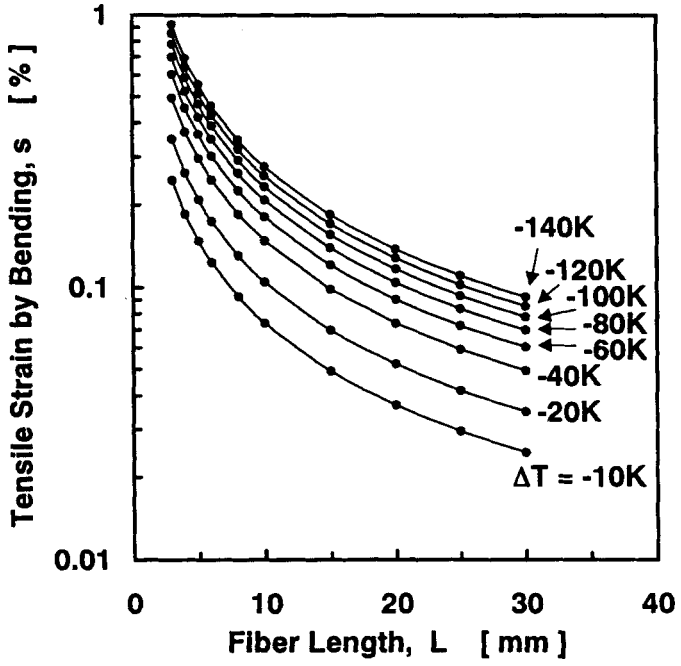

FIG. 7. A relationship between *s* and *L* replotted from Fig. 5.

The parameter n was reported to be 20 to 23 for jacketed commercial fibers [9]. Although *n* changes depending on the environment in which the fibers were treated, $n = 20$ or 23 is used in the following discussion. Using a proportional relationship between the stress σ and the strain *s*, Eq. (6) can be rewritten as

$$s_1^n t_1 = s_2^n t_2$$

$$t_1 = (s_2 / s_1)^n t_2 . \tag{6}$$

Here, when setting t_2 to be 25 yr of common device service time under residual strain s_2, one can calculate the test duration t_1 under the test strain s_1, which is equivalent to $t_2 = 25$ yr.

Figure 8 shows the calculated test duration as a function of the strain ratio $(s_2 / s_1) = (s_{(\text{service})} / s_{(\text{test})})$. Assuming the service temperature and the test temperature to be 40°C and –20°C, respectively, the ratio $(s_{(\text{service})} / s_{(\text{test})})$ is 0.63 for all fiber lengths. From Fig. 8, the test duration $t_{(\text{test})}$ corresponding to $t_{(\text{service})} = 25$ yr is derived as 5.3 h for $n = 23$ and 21 h for $n = 20$. Although this is just a rough estimate, the storage test at –20°C for a duration of several hours seems to be reasonable to simulate over 10 yr of actual device operation. The test strain, corresponding to the residual strain at –20°C, is 0.47% for the 5-mm-long fiber, 0.16% for the 15-mm-long fiber, and 0.094% for the 25-mm-long fiber.

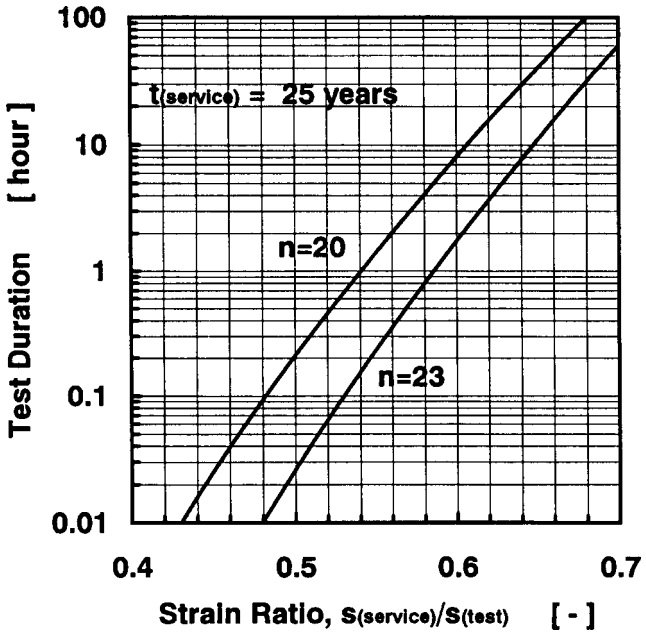

FIG. 8. Test duration calculated as a function of the strain ratio $(s_2/s_1) = (s_{(\text{service})}/s_{(\text{test})})$.

4. CONCLUSION

The proposed low-temperature storage test (e.g., at –20°C for 5 h) seems to be an effective method of screening out possible fiber break failures by intensifying the buckling deformation of assembled fibers. A combination of the low temperature storage test and the standard temperature cycle test is an alternative procedure.

REFERENCES

[1] R. S. Moyer, R. Grencavich, R. W. Smith, and W. J. Minford, "Design and qualification of hermetically packaged lithium niobate optical modulator," in *Proceedings of Electronic Component and Technology Conference*, San Jose, CA (IEEE), pp. 425-429, 1997.

[2] H. Nagata, N. Mitsugi, M. Shiroishi, T. Saito, T. Tteyama, and S. Murata, "Elimination of optical fiber breaks in stainless steel packages for $LiNbO_3$ optical modulator devices," *Opt. Fiber Technol*., vol. 2, 98 (1996).

[3] N. Mitsugi, H. Nagata, M. Shiroishi, N. Miyamoto, and R. Kaizu, "Optical fiber breaks due to buckling: problems in device packaging," *Opt. Fiber Technol*., vol. 1,278 (1995).

[4] H. Nagata and N. Mitsugi, "Mechanical reliability of $LiNbO_3$ optical modulators hermetically sealed in stainless steel packages," *Opt. Fiber Technol*., vol. 2, 216 (1996).

[5] W. R. Wagner, "Extrinsic fibcr damage and its effect on the reliability of optical fiber cormectors and splices," *Proc. SPIE*, vol. 1580, 168 (199D.

[6] E. Suhir, "Predicted curvatures and stresses in a fiber-optic interconnect subjected to bending," *J. Lig:htwave Technol*., vol. 14, 144 (1996).

[7] E. Suhir, C. Paola, and W. M. MacDonald, "Input/output fiber configuration in a laser package design," *J. Lightwave Technol*., vol. 1 1, 2087 (1993).

[8] N. Mekada, M. Seino, Y. Kubota, and H. Nakajima, "Practical method of waveguide-to-fiber connection: direct preparation of waveguide endface by cutting machine and reinforcement using ruby beads," *Appl. Opt*., vol. 29, 5096 (1990).

[9] H. Suziki, *Evaluation of Wear-Out Failures of Electronics Devices* [Denishi-Bunin no Hiro-Shinraisei Hyoka], REALIZE INC., Tokyo, pp. 172-181, 1996. [In Japanese]